

## Convective Heat Transfer in Ventilated Space with Various Partitions

**Kangyoul Bae\***

*Graduate School, Gyeongsang National University, Kyungnam 650-160, Korea*

**Hanshik Chung**

*School of Transport Vehicle Engineering, Gyeongsang National University, Kyungnam 650-160, Korea*

**Hyomin Jeong**

*School of Transport Vehicle Engineering, The Institute of Marine Industry,  
Gyeongsang National University, Kyungnam 650-160, Korea*

The laminar convective heat transfer in ventilated space with various horizontal partitions was studied numerically and experimentally. For the numerical study, the governing equations were solved by using a finite volume method for various numbers  $Re$ ,  $Gr$ ,  $Pr$  and partition numbers. The experimental study was conducted by using a holographic interferometer. The isotherms and velocity vectors have been presented for various parameters. As the number and length of partition increased, convective heat transfer decreased. Based on the numerical data, correlation equations were obtained for the mean Nusselt number in term of  $Gr/Re^2$ . In the region of  $Gr/Re^2 \leq 1$ , the mean Nusselt number was small, but in the region of  $Gr/Re^2 > 1$ , the mean Nusselt number was constant.

**Key Words :** Laminar Heat Transfer, Reynolds Number, Grashof Number, Partitions, Holographic Interferometer

### Nomenclature

$b$  : Inlet breadth of space [m]  
 $g$  : Gravity acceleration [ $m/s^2$ ]  
 $Gr$  : Grashof number  
 $h$  : Convection heat transfer factor [ $w/m^2 \cdot k$ ]  
 $k$  : Conduction heat transfer factor [ $w/m \cdot k$ ]  
 $L_p$  : Dimensionless length of partitions  
 $l_p$  : Length of partitions [m]  
 $Nu$  : Local Nusselt number  
 $\overline{Nu}$  : Mean Nusselt number  
 $\overline{Nu}_o$  : Mean Nusselt number without partition  
 $n$  : Normal coordinate to wall  
 $Pr$  : Prandtl number  
 $Re$  : Reynolds number  
 $T$  : Temperature [ $^{\circ}C$ ]

$u$  : X direction velocity [m/s]  
 $v$  : Y direction velocity [m/s]  
 $x$  : Horizontal coordinate [m]  
 $y$  : Vertical coordinate [m]  
 $\beta$  : Thermal expansion coefficient [ $K^{-1}$ ]  
 $\mu$  : Viscosity [kg/ms]  
 $\nu$  : Kinematic viscosity [ $m^2/s$ ]  
 $\theta$  : Dimensionless temperature  
 $\rho$  : density [ $kg/m^3$ ]

### Subscripts

$in$  : Inlet of space  
 $w$  : Heated wall

## 1. Introduction

Convective heat transfer in space partially divided by single or multiple dividers has received considerable affect in recent years. Ede(1976) has reported characteristic results of laminar and turbulent flow in natural convection mode and the

\* Corresponding Author,

E-mail : kybae7@yahoo.co.kr

TEL : +82-55-646-4766; FAX : +82-55-640-3188

School of Transport Vehicle Engineering, The Institute of Marine Industry, Gyeongsang National University, Kyungnam 650-160, Korea (Manuscript Received March 2, 2001; Revised January 7, 2002)

cooling performance of multichip module was reported by Choi and Cho (2000). The numerical model for a square cavity enclosure was developed and studied experimentally by Oberkampf (1976), Penot and Pavlovic (1986), Suzuki et al. (1993), Yang and Tao (1995), and Papanicolaou and Jaluria (1995). They also presented combined natural convection and radiation in a heated square enclosure and also turbulent combined free and forced convection heat transfer in an isothermal cavity. Yücel and Acharya (1991), Hanjalic et al. (1994), Chung et al. (1994) and Lakhal et al. (1994) studied heat transfer in a square enclosure with partitions and reported flow patterns, and some correlations. To improve indoor ventilation. Lee et al. (2000) has reported the ventilation effectiveness for mechanical ventilation systems with forced or natural inlet and outlet. Launder, B. (1974), Cheesewright, R. (1986) and Davidson, L. (1990) reported the flow and temperature distributions in cavity by using turbulence models.

In this research work, laminar convective heat transfer was analysed and compared with experimental data. The effects of Reynolds number, Grashof number, and the number and length of partition in the ventilated space were analyzed. And also, correlation equations with various parameters were suggested, and these equations can be used to design the heat treatment of printed circuit board and building space.

## 2. Mathematical Analysis

The governing equations for steady, two-dimensional, Navier-Stokes equations incorporating Boussinesq approximation can be written as:

Continuity:

$$\frac{\partial u}{\partial x} + \frac{\partial v}{\partial y} = 0 \quad (1)$$

Momentum:

$$\begin{aligned} & \frac{\partial(\rho u^2)}{\partial x} + \frac{\partial(\rho uv)}{\partial y} \\ & = -\frac{\partial p}{\partial x} + \mu \left( \frac{\partial^2 u}{\partial x^2} + \frac{\partial^2 u}{\partial y^2} \right) \end{aligned} \quad (2)$$

$$\begin{aligned} & \frac{\partial(\rho uv)}{\partial x} + \frac{\partial(\rho v^2)}{\partial y} \\ & = -\frac{\partial p}{\partial y} + \mu \left( \frac{\partial^2 v}{\partial x^2} + \frac{\partial^2 v}{\partial y^2} \right) + \rho g \beta \Delta T \end{aligned} \quad (3)$$

Energy:

$$\frac{\partial(uT)}{\partial x} + \frac{\partial(vT)}{\partial y} = \frac{\nu}{\text{Pr}} \left( \frac{\partial^2 T}{\partial x^2} + \frac{\partial^2 T}{\partial y^2} \right) \quad (4)$$

The discretization method used to solve the differential equations is a control volume approach. The discretization scheme used for convection-diffusion formulation is a hybrid scheme. The SIMPLE solution procedure with a line-by-line method, a staggered grid, and under-relaxation was used in this study. As the convergence condition, the total grid errors in mass flow rate of under 0.3% was adopted.

Two dimensional grid number is  $80 \times 80$ , and the boundary conditions were as follows.

$$\text{Inlet : } u = U_{in}, v = 0, T = T_{in} \quad (5)$$

$$\text{Outlet : } \frac{\partial v}{\partial y} = 0, u = 0, \frac{\partial T}{\partial y} = 0 \quad (6)$$

$$\text{Heated surface (bottom wall) : } T = T_w \quad (7)$$

$$\text{Isothermal surface and partitions : } \frac{\partial T}{\partial n} = 0 \quad (8)$$

The following dimensionless quantities were introduced

$$X = \frac{x}{b}, Y = \frac{y}{b}, U = \frac{u}{U_{in}}, V = \frac{v}{U_{in}} \quad (9)$$

$$\theta = \frac{T - T_{in}}{T_w - T_{in}} \quad (10)$$

$$Gr = \frac{g \beta (T_w - T_{in}) b^3}{\nu^2} \quad (11)$$

$$Re = \frac{\rho b U_{in}}{\mu} \quad (12)$$

$$L_p = \frac{l_p}{b} \quad (13)$$

The size of partition thickness is one half of inlet breadth, and the local Nusselt number  $Nu$  and the mean Nusselt number  $\overline{Nu}$  were calculated as follows.

• local Nusselt number :

$$Nu = \frac{hL}{k} = -\frac{\partial \theta}{\partial Y} \Big|_{Y=0} \quad (14)$$

• mean Nusselt number :

$$\overline{Nu} = \frac{1}{L} \int Nu \cdot dx \quad (15)$$

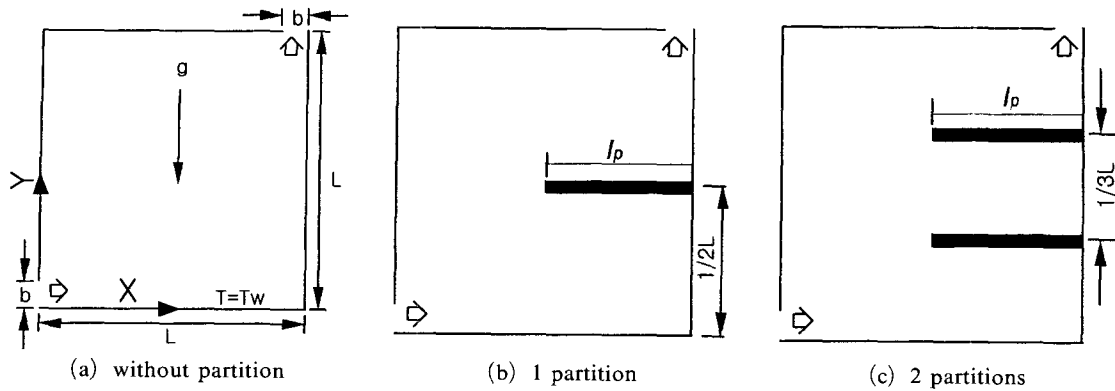


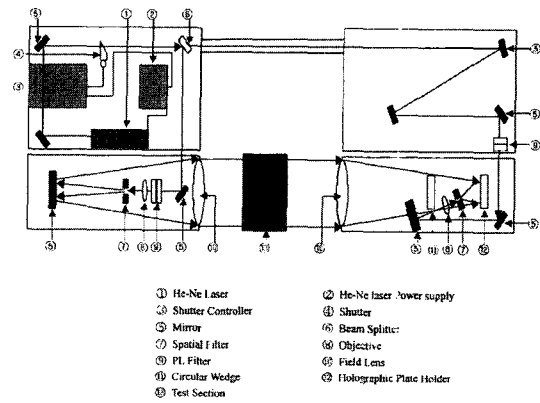
Fig. 1 Schematic diagram for present study

The geometry for numerical study are shown schematically in Fig. 1. Air enters from the lower inlet of the left wall with temperature  $T_{in}$  and uniform velocity  $U_{in}$  and flows out through the upper outlet. The bottom surface is maintained at  $T_w$ , and the other surfaces are adiabatic. Three different cases were considered without partition; 1-partition; and 2-partitions with inlet and outlet size of  $1/10L$ .

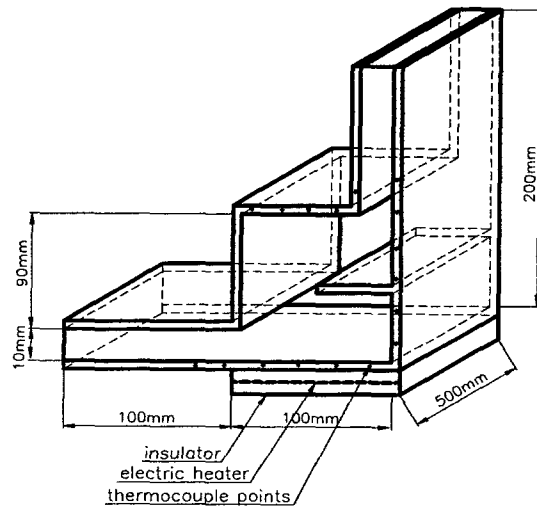
### 3. Results & Discussion

Figure 2(a) and (b) show schematic diagram of holographic interferometer and the details of the test section. The test section with an inlet and an outlet were made of 10mm-thick bakelite. The inlet velocity was measured by a hot-wire anemometer. The temperature measurement was conducted by using a T-type thermocouple, a hybrid recorder and a PC. A holographic interferometer was used for visualization as shown in Fig. 2(b).

The experimental and numerical results are compared in Fig. 3. The velocity and temperature difference are 0.3m/s and  $\Delta T=20$ , respectively. In the cases of 1-partition and no partition, the calculation and experiment showed a good agreement. However, of the 2-partition case, there were some differences between the calculation and the experiment. Numerical and experimental errors may have resulted from the constant property assumption, the neglect of radiation heat transfer, optical problem, and the imperfect



(a) Schematic diagram of Holographic Interferometer



(b) The 1-partition test section of experimental study

Fig. 2 Schematic diagram and test section

insulation. However the qualitative agreement of two results were favorable. The local Nusselt

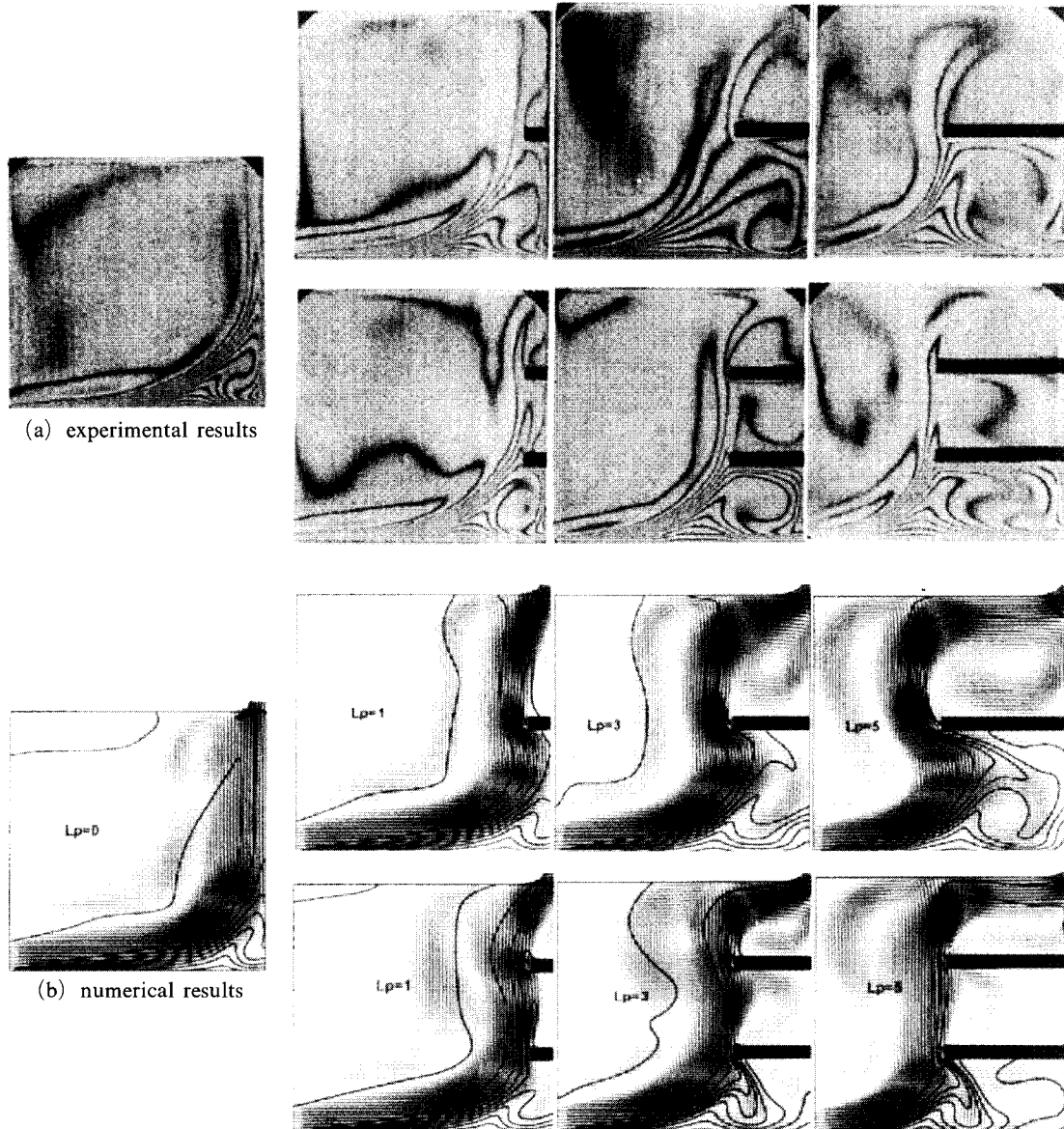


Fig. 3 Comparison with numerical and experimental results at  $Re \approx 200$ ,  $Gr \approx 2870$ ,  $Pr \approx 0.71$

numbers on a heating surface are represented in Fig. 4 and Fig. 5 for various lengths ( $L_p$ ) with  $Gr/Re^2 = 8 \times 10^{-4}$ ,  $9 \times 10^{-3}$  and 5.3. The local Nusselt numbers decreased for  $4 < X < 6$  as shown Fig. 4(a). But, in the region of  $X > 8$ , the Nusselt number increased because of a velocity recirculation attachment area as shown in Fig. 3. In these Fings, the horizontal  $X$  value represents the dimensionless value of  $L/b$ . As the length of partition increases, the position  $X$  for the mini-

mum Nusselt number became short because of the flow separation point as shown in Fig. 3. But, for a large  $Gr/Re^2$  as shown in Fig. 4(c), the heat transfer was not influenced by the partition length, and this area coincided with constant room temperature area as shown in Fig. 6.

Figure 5 represents the local Nusselt number on a heating surface for the 2-partitions case. The local Nusselt number distributions is similar to the 1-partition, case.

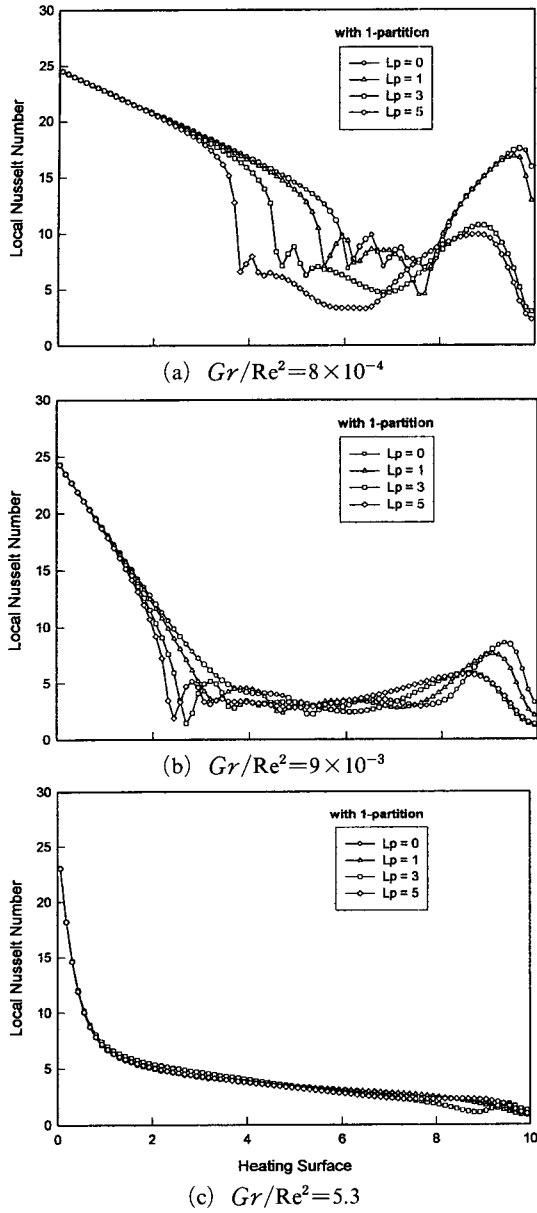


Fig. 4 The distributions of local Nusselt number on a heating surface in case of 1-partition

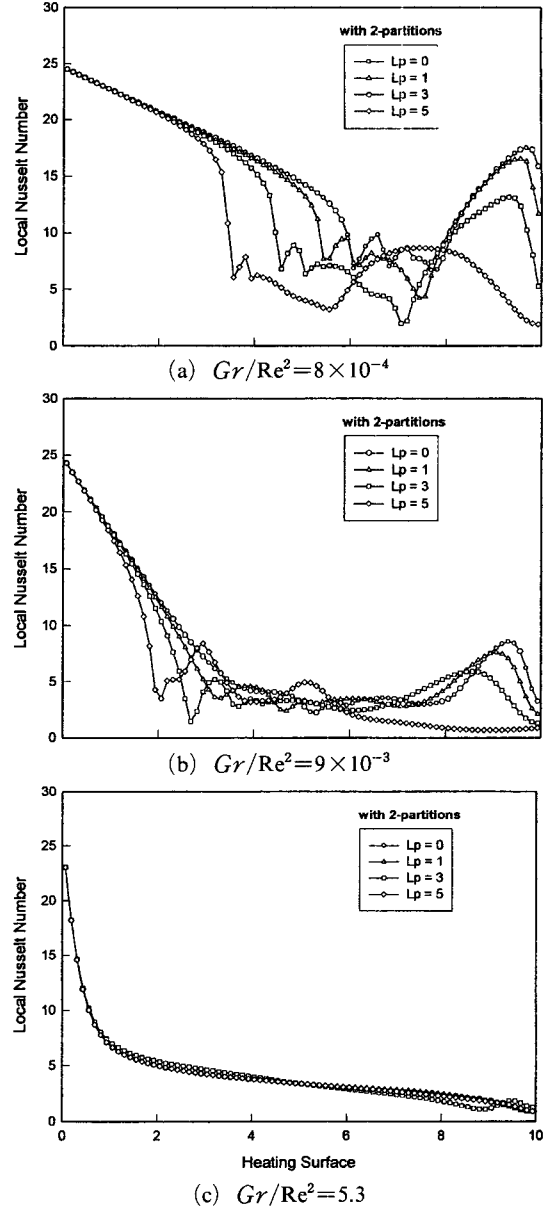


Fig. 5 The distributions of local Nusselt number at a heating surface in case of 2-partition

Generally, as the length and number of partitions increase, the convective heat transfer decreases. The small cell can be found under the partition as the length and number of partitions increase. The cell decreased heat transfer because the hot air cell from the heating wall stagnated under the partition. Judging from the velocity vectors obtained from the numerical solution, a

recirculation area appeared under the partition, and a strong recirculation cell was formed by increasing the length and the number of partitions.

In the cases of 1-partition and 2-partitions, the dimensionless mean room temperature versus  $Gr/Re^2$  for various partition lengths is shown in Fig. 6. The vertical axis shows a dimensionless

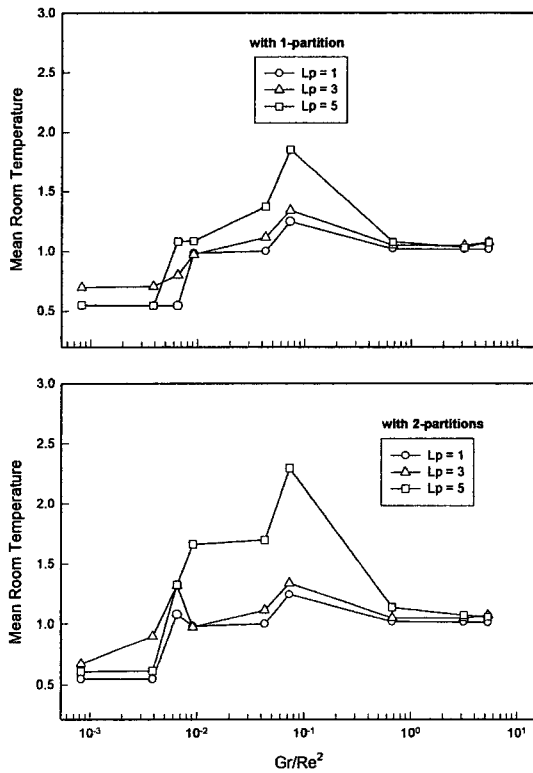


Fig. 6 The mean room temperature versus  $Gr/Re^2$  for various length of partition

mean room temperature nomaliquedly the a mean room temperature in the no partition case. The peak mean room temperature can be found at  $Gr/Re^2=0.1$  in the 1-partition case for  $L_P=1, 3$  and  $5$ . However, the peak mean room temperature can be found at  $Gr/Re^2=6 \times 10^{-3}$  for  $L_P=3$ , and  $Gr/Re^2=0.1$  for  $L_P=1, 5$  in 2-partition case. These results show that the longer length of partition increases the room temperature.

The mean Nusselt number  $\overline{Nu}/Nu_0$  versus  $Gr/Re^2$  for various lengths of 1-partition and 2-partitions is shown in Fig. 7. At  $Gr/Re^2 > 1$ , the mean Nusselt numbers for all cases converge to the same value. These results imply that the length and the number of partition have no effect on the heat transfer rate. However, in the region of  $Gr/Re^2 < 1$ , the heat transfer rate decreased very rapidly with the partition length.

From the numerical results, the correlation for  $\overline{Nu}/Nu_0$  is shown Eq. (9) and the corresponding constants are given in Table 1.

Table 1 Constants for  $\overline{Nu}/Nu_0 = a \cdot (Gr/Re^2)^b$

Partition number	Partition length $L_p$	Constants	
		a	b
1	1	0.984	0.027
	2	0.977	0.058
	3	0.966	0.075
2	1	0.985	0.013
	2	0.972	0.054
	3	0.964	0.089

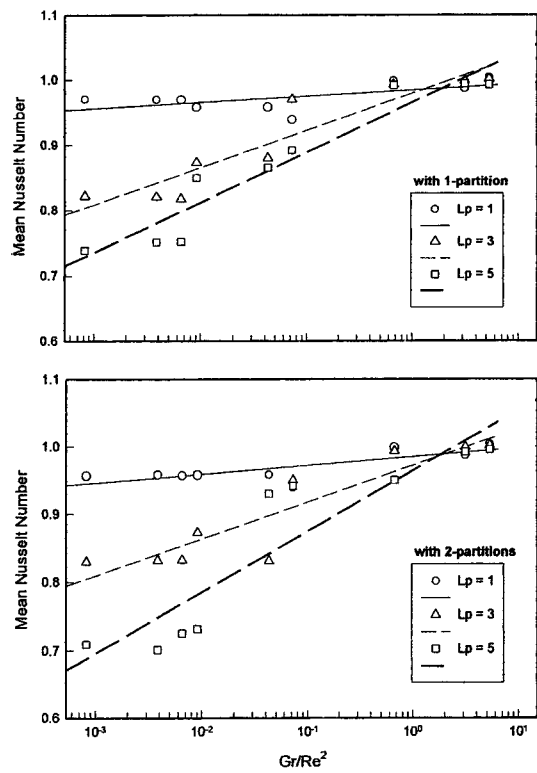


Fig. 7 The mean Nusselt number versus  $Gr/Re^2$  for various length of partition

$$\frac{\overline{Nu}}{Nu_0} = a \cdot \left(\frac{Gr}{Re^2}\right)^b \quad (16)$$

#### 4. Conclusions

Natural convective heat transfer in ventilated space with horizontal partitions have been studied numerically and experimentally.

(1) As the number and length of partitions increase, the convective heat transfer rate de-

creased.

(2) A comparison of experimental and numerical isotherms showed qualitatively good agreement in case of 1-partition and without partition. However, there was some difference in the 2-partition case when  $L_p$  was great than 3.

(3) The heat transfer rate was ruoe strongly influenced by the partition length than by the number of partitions.

(4) For  $Gr/Re^2 > 1$ , the mean Nusselt number and mean room temperature had no relations to the length and number of partitions.

(5) From the numerical results, a correlation was obtained for the mean Nusselt number in terms of  $Gr/Re^2$ .

### Acknowledgements

This work was supported by the Brain Korea 21 Project, and the authors gratefully appreciate the support.

### References

- Cheesewright, R., King, K. J. and Ziai, S., 1986, "Experimental data of the Validation of Computer Codes for the Prediction of Two Dimensional Buoyancy Cavity Flow," *Significant Questions in Buoyancy Affected Enclosure or Cavity Flows, ASME-HTD*, pp. 75~81.
- Choi, M. and Cho, K., 2000, "Influence of an Aspect Ratio of Rectangular Channel on the Cooling Performance of a Multichip Module," *KSME Int. J.*, Vol. 14, No. 3, pp. 350~357.
- Chung, H., Jeong, H., Lee, C. and Kwon, S., 1998, "Study on Convection Heat Transfer in a Ventilated Room with Horizontal Partitions," *Proc. of 11<sup>th</sup> IHTC*, Vol. 3, pp. 245~250.
- Davidson, L., 1990, "Calculation of the Turbulent Buoyancy-Driven Flow in a Rectangular Cavity Using an Efficient Solver and Two Different Low Reynolds Number  $k-\epsilon$  Turbulence Models," *Numerical Heat Transfer*, Vol. 18, Part A, pp. 129~147.
- Ede, A. J., 1976, "Advances in Free Convection," *Advances in Heat Transfer, Academic Press, New York*, pp. 1~64.
- Hanjalic, K., Kenjeres, S. and Durst, F., 1994, "Numerical Study of Natural Convection in Partitioned 2-Dimensional Enclosures at Transition Rayleigh Numbers," *Proc. 10<sup>th</sup> Int. Heat Transfer Cong., Brighton*, Vol. 7, pp. 97~102.
- Lakhal, E. K., Hasnaoui, M., Bilgen, E. and Vasseur, P., 1994, "Natural Convection Heat Transfer in Rectangular Enclosures with Perfectly Conduction Fins Attached on the Heated Wall," *Proc. 10<sup>th</sup> Int. Heat Transfer Cong., Brighton*, Vol. 7, pp. 97~102.
- Launder, B. E. and Sharma, B. I., 1974, "Application of the Energy-Dissipation Model of Turbulence to the Calculation of Flow Near a Spinning Disc," *Letters in Heat and Mass Transfer*, vol. 1, pp. 131~138.
- Lee, J., Kang, T., Lee, K., Cho, M., Shin, J., Kim S., Koo, J. and Lee, J., 2000, "An Experimental Study of Ventilation Effectiveness in Mechanical Ventilation Systems using a Tracer Gas Method," *KSME Int. J.*, Vol. 14, No. 11, pp. 1286~1295.
- Oberkampf, W. L. and Crow, L. I., 1976, "Numerical Study of the Velocity and Temperature Field in a Flow-Through Reservoir," *Journal of Heat Transfer, ASME*, pp. 353~359.
- Papanicolaou, E. and Jaluria, Y., 1995, "Computation of Turbulent Flow in Mixed Convection in a Cavity with a Localized Heat Source," *Journal of Heat Transfer, ASME*, Vol. 117, pp. 649~658.
- Penot, F. and Pavlovic, M., 1986, "Heat Transfer Analysis of Mixed Convection in a Heated Cavity," *Proc. 8<sup>th</sup> Int. Heat Transfer Conf., San Francisco*, Vol. 3, pp. 1419~1424.
- Susuki, H., Hasegawa, E. and Matsufuji, H., 1993, "Motion of Small Particles due to a Pulsatile Flow in a Chamber," *ASME International Journal Series N*, Vol. 36, No. 1, pp. 57~65.
- Yang, M. and Tao, W. Q., 1995, "Three-Dimensional Natural Convection in an enclosure with an Internal Isolated Vertical Plate," *Journal of Heat Transfer, ASME*, Vol. 117, pp. 619~625.
- Yucel, A. and Acharya, S., 1991, "Natural Convection of a Radiating Fluid in a Partially Divided Square Enclosure," *Numerical Heat Transfer, Part A*, Vol. 19, pp. 417~485.